Computers and Structures 89 (2011) 959–967

Contents lists available at ScienceDirect

Computers and Structures

journal homepage: www.elsevier.com/locate/compstruc

Numerical and experimental evaluation of seismic capacity of high-rise steel buildings subjected to long duration earthquakes

D.G. Lignos [a,*], Y. Chung [b], T. Nagae [c], M. Nakashima [d]

[a] Department of Civil Engineering and Applied Mechanics, McGill University, 817 Sherbrooke St. West, Room 278C, Montreal QC, Canada H3A 2K6
[b] Division of Seismic Resistant Structures, Disaster Prevention Research Institute (DPRI), Kyoto University, #S301D Gokasho, Uji, Kyoto 611-0011, Japan
[c] National Research Institute for Earth Science and Disaster Prevention, Miki, Hyogo 673-0515, Japan
[d] Division of Seismic Resistant Structures, Disaster Prevention Research Institute (DPRI), Kyoto University, #S307D Gokasho, Uji, Kyoto 611-0011, Japan

ARTICLE INFO

Article history:
Received 2 July 2010
Accepted 25 January 2011
Available online 18 February 2011

Keywords:
High-rise
Fracture
Cumulative damage
Long duration
Low cycle fatigue
Post-fracture seismic capacity

ABSTRACT

Occurrences of large earthquakes having a magnitude larger than eight along subduction zones have been reported worldwide. Due to large number of load reversals the effect of cumulative damage on structural components due to deterioration becomes critical for steel buildings of old construction but may also become critical for buildings designed based on current seismic provisions. A state-of-the-art analytical model that simulates component deterioration and fracture due to low cycle fatigue has been developed and implemented in the OpenSees computational framework. The model serves for seismic evaluation of steel moment frame structures subjected to long duration records. The effectiveness of the numerical model in quantification of the seismic capacity of high rise steel structures is demonstrated through validation with a full scale shaking table test of a high-rise steel building subjected to a long duration record at the world's largest shaking table facility (E-Defense). Limitations of the proposed numerical model are also discussed.

© 2011 Elsevier Ltd. All rights reserved.

1. Introduction

Recent earthquakes around the world (Northridge, 1994; Kobe, 1995) raised many concerns regarding the seismic performance of steel moment resisting frames (MRF) due to the occurrence of brittle fractures of welded beam-to-column connections [1,2]. Various analytical studies [3–6] summarized the effect of brittle fractures on seismic capacity of existing steel moment frames. This forced the earthquake engineering community to design improved steel connections so that brittle fracture is avoided [7,8].

However, improved steel moment connections may not be invincible when subjected to a large number of inelastic cycles due to low cycle fatigue [9–14]. This is more evident in high-rise steel buildings that are subjected to long period long duration ground motions that occur near subduction zones. The reason is that the predominant period of these ground motions range from several to 10 s, and their primary durations extend over several minutes [15–17]. These ground motions tend to resonate high-rise buildings whose fundamental natural periods are above 2 s. This observation was confirmed by recent full-scale shake table tests that represented typical high-rise construction in Japan [18]. These tests took place at the world's largest shake table facility at E-Defense. Prior numerical studies [19] on high-rise steel buildings subjected to long period long duration ground motions also confirmed the same observation.

During the past years a large number of numerical and experimental studies emphasized on the importance of fracture on the seismic capacity of steel MRF due to seismic loading. Nakashima et al. [20] investigated the effect of moment redistribution caused by beam fracture in steel MRF based on static loading. The main conclusion of this study was that sequential fractures are less likely to occur during static moment redistribution when rotations corresponding to fracture are large. Utilizing a large number of steel MRFs as part of the SAC phase II project in United States, Luco and Cornell [21] investigated the effect of connection brittle fractures on seismic drift demands of steel MRFs using an empirical analysis model to assess brittle fracture. They concluded that the effects of connection fractures are more pronounced at higher drift demand levels.

Rodgers and Mahin [22] demonstrated both experimentally and numerically that severe strength loss due to the combination of numerous fractures in steel MRFs and large excitation can have adverse consequences, including collapse. Nakashima et al. [23] investigated experimentally the effect of residual strength of a steel MRF on connection fractures. The composite effect due to slab

* Corresponding author. Tel.: +1 514 398 2198; fax: +1 514 398 7361.
E-mail addresses: dimitrios.lignos@mcgill.ca (D.G. Lignos), yulin.chung@ks7.ecs.kyoto-u.ac.jp (Y. Chung), nagae@bosai.go.jp (T. Nagae), nakashima@archi.kyoto-u.ac.jp (M. Nakashima).

0045-7949/$ - see front matter © 2011 Elsevier Ltd. All rights reserved.
doi:10.1016/j.compstruc.2011.01.017

on connection fractures was also assessed in this study. They concluded that after fracture of the bottom flange of a steel beam due to slab effect occurs, the residual capacity of composite steel MRFs is about 35% of the respective maximum strength at relatively large drifts. Recent full scale shaking tables on high-rise steel buildings conducted on the world's largest shaking table at E-Defense [10,18,24] demonstrated the vulnerability of steel beam-to-column connections to long period long duration ground motions. In these connections, fracture occurs due to the large number of inelastic deformations resulting to severe strength deterioration.

Consequently, there is a need to investigate the effect of component deterioration and ductile fracture on the seismic capacity of high-rise steel buildings. This will contribute to effective decisions on retrofit techniques for steel beam-to-column connections. For this purpose, a numerical model that is able to simulate complex deterioration phenomena and ultimately connection fracture due to low cycle fatigue has been developed and implemented in the Open System for Earthquake Engineering Simulation (openSees) platform [25], which is available from the Pacific Earthquake Engineering Research Center (PEER). The component model has been calibrated against a large number of steel component tests that have been conducted over the past years around the world. The validity of the numerical model is demonstrated with recently conducted full scale shaking table test of a high-rise steel building [18,24]. This test took place at the E-Defense facility in Japan. The seismic capacity of the high-rise steel structure after the occurrence of connection fractures is evaluated numerically after utilizing the same numerical model. Limitations of the proposed numerical model are also summarized at the end of this paper.

2. Numerical model for prediction of fracture due to low cycle fatigue

Various models have been proposed to investigate the effect of low cycle fatigue on steel beam-to-column connections. Bertero and Popov [26] derived a relationship between plastic strain amplitude and the number of cycles to fracture based on strain-controlled tests that lead to fracture of steel beam flanges after severe local buckling. Park et al. [27] incorporated the maximum deformation and energy dissipation due to hysteresis in a damage index. More recently, Krawinkler et al. [28] developed a numerical model that can simulate the effect of cumulative damage due to earthquake excitations based on Coffin–Manson [29] relationship considering the full loading history of a steel component subjected to cyclic loading.

For prediction of inelastic buckling and fracture of steel braces due to low cycle fatigue, a distributed plasticity model [30] that incorporates rainflow counting was developed and validated with experimental data of steel braces. Krishnan [31] developed an elastofiber element that can simulate inelastic post-buckling response including fracture of steel braces and slender columns. Kanvinde et al. [32–34] proposed and demonstrated the effectiveness of a cyclic void growth model (VGI) to assess ductile fracture initiation due to low cycle fatigue for steel connections and steel braces. Lin et al. [35] utilized the VGI model in detailed finite element studies for prediction of fracture initiation of field welded steel connections. Lee and Stojadinovic [36] developed a new cyclic yield-line plastic hinge model for estimating connection rotation capacity. This model is applicable by designers to evaluate new steel connections before required proof of performance tests. Campbell et al. [37] presented a summary of damage predictions in steel MRFs under earthquakes in which low cycle fatigue is incorporated based on a compilation of salient analytical and experimental results.

This paper focuses on the capability of simulating component deterioration and fracture due low cycle fatigue with an inelastic concentrated plasticity element that was recently implemented in the OpenSees computational framework [25] (http://opensees.berkeley.edu). In particular, a fracture rule was incorporated in the modified Ibarra–Krawinkler deterioration model [38,39] that allows modeling of (1) strength and stiffness deterioration and (2) rupture leading to complete severing of a steel beam-to-column connection due to cyclic loading. This analytical model serves for seismic evaluation of steel MRFs at extreme seismic loading, including the quantification of post-fracture response. The emphasis is on high-rise steel buildings subjected to long period long duration ground motions. Because of the large number loading reversals in these ground motions, steel connections deteriorate cyclically in strength and stiffness and ultimately fracture due to low cycle fatigue.

2.1. Component deterioration modeling

The modified Ibarra–Krawinkler phenomenological analytical model is able to simulate stiffness and strength component deterioration by using a reference backbone curve shown in Fig. 1a. To control cyclic deterioration, an energy-based rule proposed by Rahnama and Krawinkler [40] is used. The hysteretic response of the modified Ibarra–Krawinkler model has been calibrated extensively during the last few years by utilizing a steel component database for deterioration modeling. This database includes tests for more than 300 steel beams [39,41]. Fig. 1a shows an example of calibration of the elastic stiffness K_e, pre- and post-capping (after local buckling occurs) rotation θ_p, θ_{pc} of a steel beam subjected to monotonic loading. The modified Ibarra–Krawinkler model deteriorates cyclically using a deterioration parameter Λ. This parameter is a reference energy dissipation capacity of a steel component that controls strength, stiffness and post-capping strength deterioration modes (see Fig. 1b). A detailed description about the original and modified Ibarra–Krawinkler deterioration model can be found in [38,39].

2.2. Modeling of fracture due to low cycle fatigue

In order to incorporate low cycle fatigue in the numerical model discussed in Section 2.1, a fracture law was implemented. For a steel component, the number of cycles to fracture N_f is expressed as a function of cumulative energy dissipation E_d of the steel component when subjected to cyclic loading. This expression can be written according to Eq. (1),

$$N_f = a_1 E_d^{-k} \tag{1}$$

This relationship is analogous to the Coffin–Manson [29] equation for low-cycle fatigue simulation,

$$N_f = b \Delta\varepsilon_p^{-a} \tag{2}$$

where $\Delta\varepsilon_p$ is the amplitude of plastic strain of a steel component. The difference between Eqs. (1) and (2) is that instead of the amplitude of plastic strain of the steel component, the dissipated hysteretic energy is expressed with respect to the number of cycles to fracture N_f. The logarithmic expression of Eq. (1) is given by,

$$\log N_f = \log(a_1) - k\log(E_d) \tag{3}$$

Eq. (3) is further simplified by,

$$\log N_f = A - k\log(E_d) \tag{4}$$

The parameters A and k in Eq. (4) depend on the loading history that a steel component experiences as part of a structure subjected to an earthquake. Fig. 2 shows the effect of two different loading histories on the parameters A and k. The two protocols that are used are a standard symmetric loading protocol and a near-fault loading

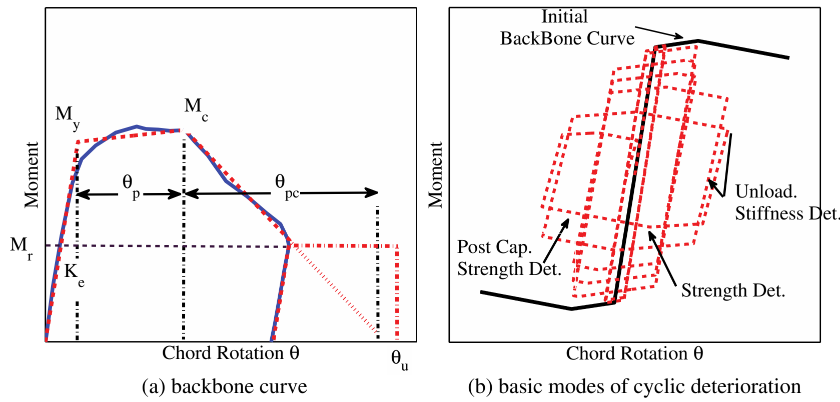

Fig. 1. Modified Ibarra–Krawinkler deterioration model (Lignos and Krawinkler [39]).

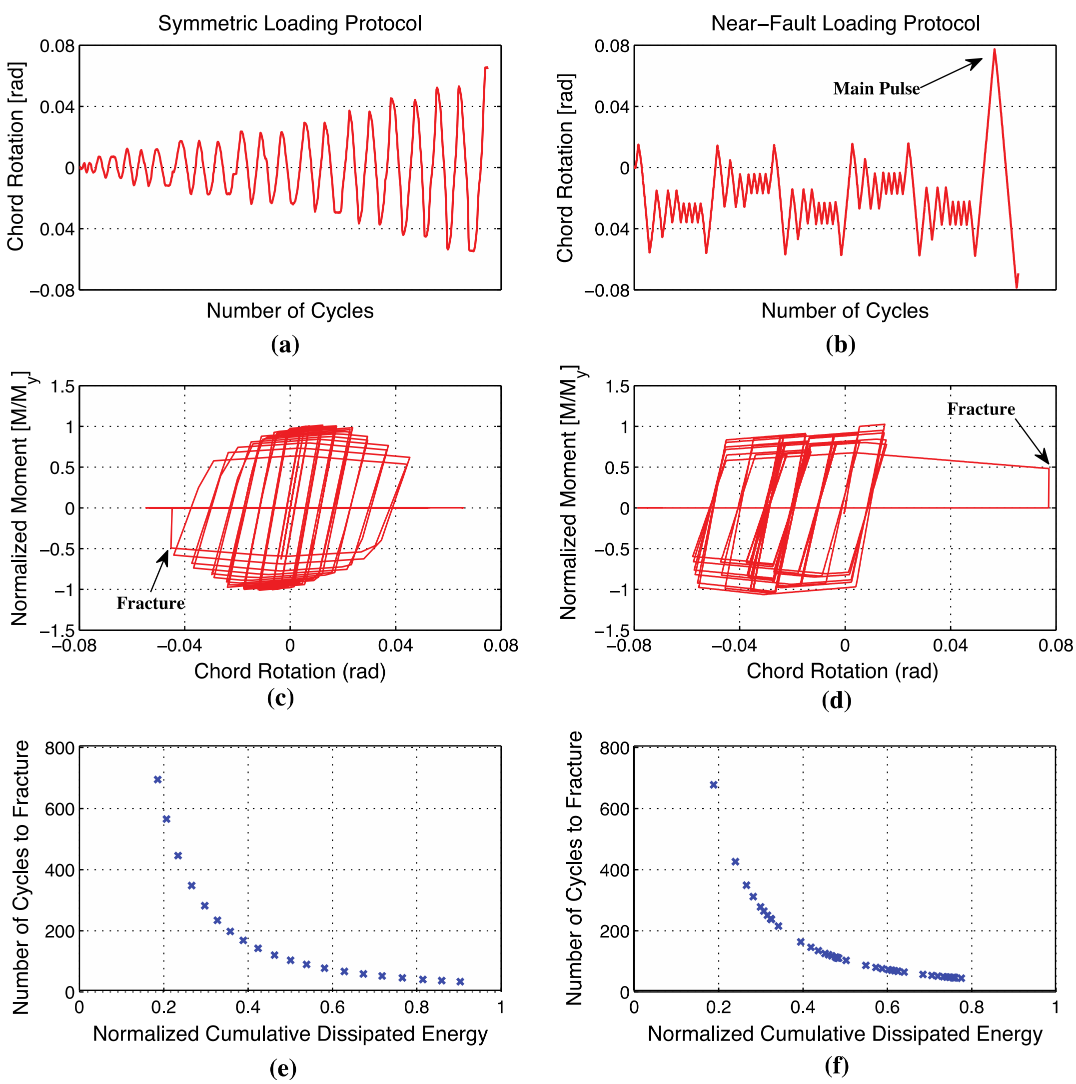

Fig. 2. Effect of loading history on fracture due to low cycle fatigue (a) symmetric loading protocol; (b) near-fault loading protocol; (c) hysteretic response due to symmetric loading protocol; (d) hysteretic response due to near-fault loading protocol; (e) cycles to fracture versus normalized cumulative dissipated energy due to symmetric loading protocol; (f) cycles to fracture versus normalized cumulative dissipated energy due to near-fault loading protocol.

protocol [42] (see Fig. 2a and b). The same steel-beam-to-column connection is used in both examples (i.e. the set of A and k parameters is identical for both cases). When a symmetric loading protocol with increased inelastic cycles is utilized, the steel component fractures at a chord rotation of about 4.4% (see Fig. 2c). In the case of the near-fault loading protocol, the same component fractures at about 8% chord rotation (see Fig. 2d). Due to the small amplitude of inelastic cycles prior to the main pulse of the near-fault protocol (see Fig. 2b) the steel component does not dissipate much energy; thus it does not fracture. The same observation can be seen from

Fig. 2e and f. These figures show the number of inelastic cycles to fracture versus the dissipated energy of the same steel component subjected to the symmetric and near-fault loading protocol, respectively. In these figures the dissipated energy of the steel component is normalized with respect to its plastic moment capacity.

The parameters A and k are calibrated with available experimental data from a steel component database for deterioration modeling [36]. Forty-three test specimens with different beam sizes were utilized in order to calibrate the two parameters (A, k) for fracture simulation of Welded Unreinforced Flange (WUF) connections. An example of this connection type is shown in Fig. 3a [43]. The calibration of the parameters A and k is based on nonlinear least-square optimization [44] using the Levenberg–Marquardt algorithm [45]. The objective function that was used was the difference between the simulated and measured bending strength at a given beam rotation. Based on the steel component tests that were used to calibrate the parameters A and k, it is concluded that a constant k may be used to represent steel components that fail in a ductile manner. A larger A value implies that a steel component is more ductile compared to another one with smaller A, i.e., the component is able to dissipate more energy prior to fracture. Kuwamura and Takagi [46] reached to the same conclusion. In their assessment, they related the number of cycles to fracture of a steel component with its cumulative plastic strain normalized with respect to the yield strain. The steel specimens that are considered for calibration of the numerical model discussed in this paper all fail in a ductile manner (fracture due to low cycle fatigue). Cases that steel beam-to-column connections fail in a brittle manner (e.g. pre-Northridge connections) is not part of this data set since the focus of this paper is to evaluate the seismic capacity of high-rise steel buildings due to large number of inelastic cycles prior to fracture. However, based on [46] a similar expression with Eq. (2) is applicable for brittle fracture simulation. An example of calibration of the simulated response of a WUF steel connection is shown in Fig. 3b. This figure indicates a relatively good match between simulated and experimental hysteretic response of a WUF connection including fracture. Fig. 4a and b shows the bending strength and unloading stiffness deterioration per cycle of the same steel component for both loading directions, respectively. From these figures it can be seen that there are four ranges of deterioration with respect to number of cycles. During the first range, there is no indication of local buckling; during the second range, deterioration occurs at a high rate associated with the continuous growth of local buckles; during the third range deterioration occurs at constant rate due to the stabilization in buckle size and during the last range, deterioration occurs due to crack propagation at the welds or buckles. Earlier experimental studies [28] have reached to the same conclusions regarding the effect of cyclic loading on component deterioration and fracture due to low cycle fatigue.

(a) WUF connection (Figure from Lignos and Billington [18])

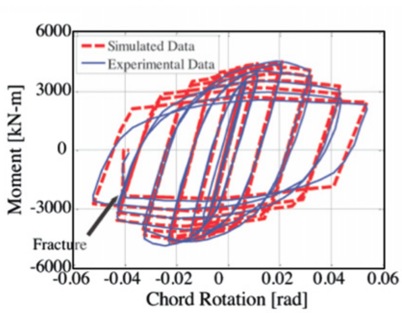

(b) experimental versus simulated hysteretic response of a WUF connection

Fig. 3. Welded Unreinforced Flange (WUF) connection. Simulated versus experimental hysteretic response of a WUF connection (experimental data from Ricles et al. [13]).

Fig. 4c shows the cumulative dissipated hysteretic energy versus the number of inelastic cycles of the same steel component that is shown in Fig. 3b. In this figure, the cumulative dissipated energy is normalized with respect to the plastic bending strength of the steel component. Fig. 4d shows the relationship of dissipated hysteretic energy versus number of cycles to fracture in logarithmic scale for the set of specimens used from [39,41]. This relationship is close to linear (linear regression coefficient $R^2 = 0.86$), which is in accordance with Eq. (5).

3. Benchmark high-rise building for validation of the numerical model

In order to validate the ability of the modified Ibarra–Krawinkler deterioration model with low cycle fatigue to predict steel connection fractures, we utilized the experimental data from a recently conducted full scale shaking table test of a steel building (see Fig. 5a). This specimen represents a prototype 21-story steel building built in Japan in 1970s. The structure was tested at the world's largest earthquake simulator facility at E-Defense in Japan [18,24]. This earthquake simulator can accommodate a specimen up to a weight of 1200 metric tons and a height of 22 m (see [24]). Hence the concept adopted for the test was to establish a partial frame structure with full-scale steel members that would be able to reproduce the possible seismic responses of the prototype. The first 4-stories of the equivalent test specimen represented the bottom stories of the prototype 21-story structure. Three concrete substitute layers represented the mass and stiffness of the remaining stories. These layers were connected with rubber bearings placed on top of the structure. The layers and rubber bearings were tuned in such a way to represent the total mass and lateral stiffness of every 5-stories of the upper portion of the 21-story prototype steel structure. A steel damper was placed at the centroid of each concrete layer to reproduce possible nonlinearity and energy dissipation of the upper stories of the prototype structure. The geometry and structural sections of the test specimen is shown in Fig. 5b. It was proven both analytically and experimentally (see [18,24]) that the test specimen represented well the response of the prototype structure. A total of 678 channels of data acquisition were used during the earthquake simulator test. Based on white noise tests prior to the testing program, the first three periods of vibration of the test frame in the longitudinal direction (see Fig. 5b) were 2.13 s, 0.80 s and 0.53 s. The first three damping ratios in the same loading direction were 2.6%, 3.4% and 4.7%. Detailed information regarding the test setup and specimen can be found in [18].

3.1. Testing program

The test specimen shown in Fig. 5 was subjected to a sequence of ordinary and long period long duration ground motions that represented design Levels 2–3 in Japanese seismic design including

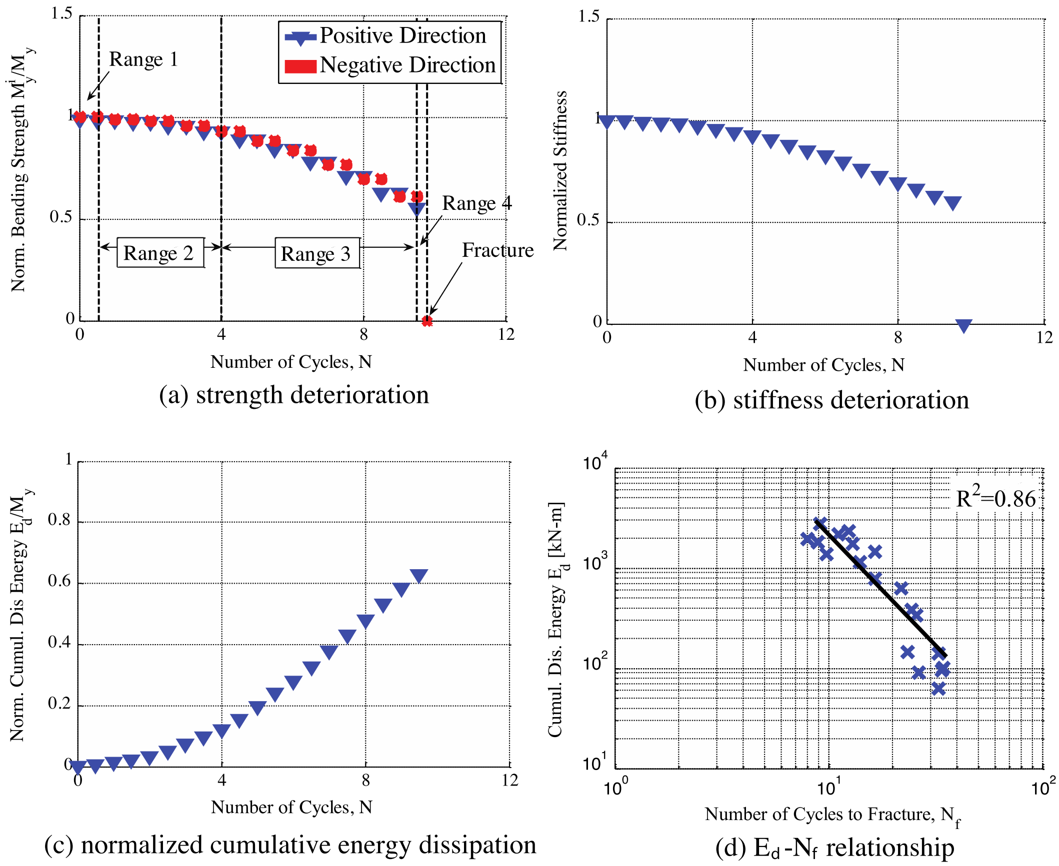

(a) strength deterioration (b) stiffness deterioration
(c) normalized cumulative energy dissipation (d) E_d-N_f relationship

Fig. 4. Effect of cumulative damage on component hysteretic behavior of steel beams.

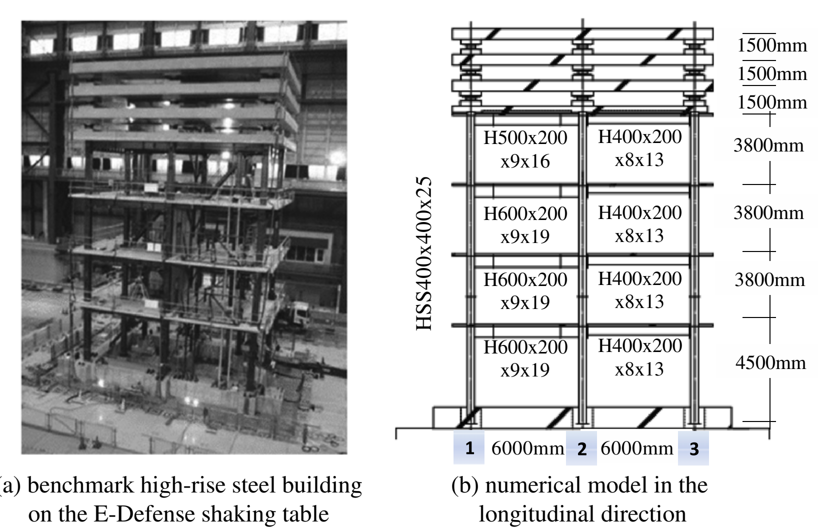

(a) benchmark high-rise steel building on the E-Defense shaking table (b) numerical model in the longitudinal direction

Fig. 5. Benchmark high-rise steel building and analytical model in the longitudinal direction.

ElCentro, Hog and three times the San wave. These motions were applied to the structure sequentially. The Hog and San seismic waves are synthesized long period long duration ground motions that are often used in recent research in Japan on the effects of such ground motions on steel structures [10,18,24]. These two waves have a predominant period of about three seconds and durations of 200 and 320 s, respectively. The Hog wave was predicted at the Kawasaki site near Tokyo (PGA = 145 cm/s^2, PGV = 40 cm/s). The San wave was predicted at a Nagoya site (PGA = 186 cm/s^2, PGV = 51 cm/s). Fig. 6 shows the acceleration and velocity spectrum of both ground motions in comparison with an ordinary ground motion such as ElCentro. More information about the two motions can be found in [18,24].

4. Numerical modeling of the test specimen and verification

A two dimensional numerical model of the steel MRF in the longitudinal loading direction was built in the OpenSees simulation

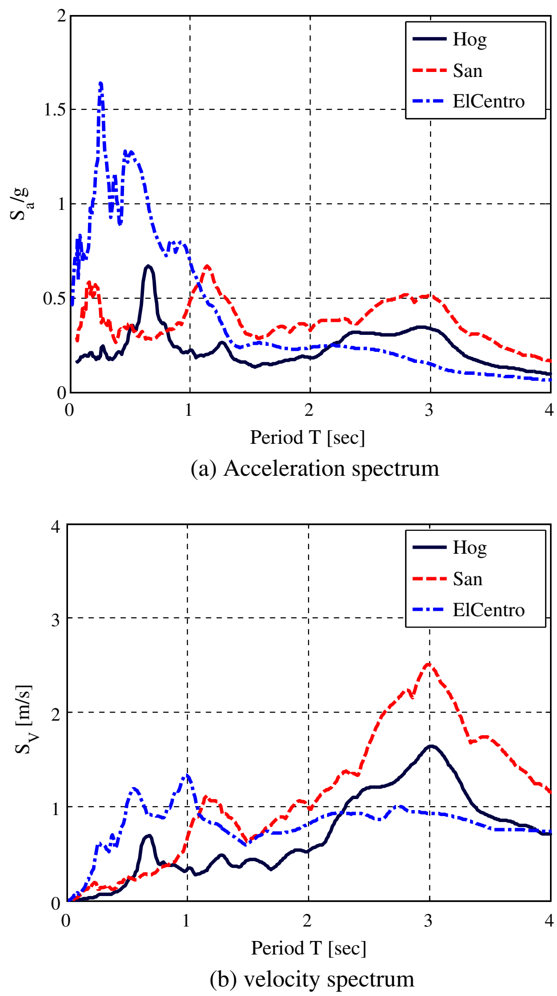

Fig. 6. Acceleration and velocity spectrum of ElCentro, Hog and San seismic waves.

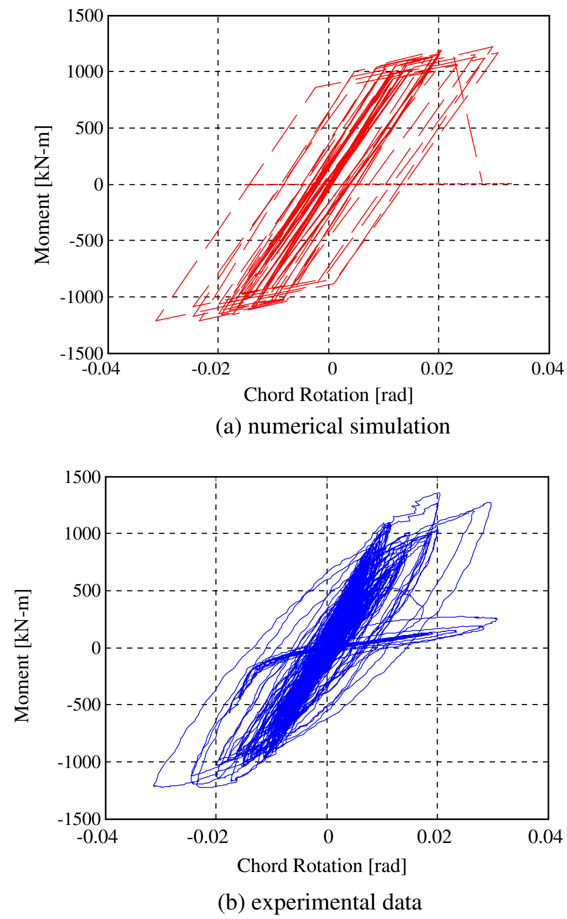

Fig. 7. Simulated versus experimental data for steel beam-to-column subassembly (experimental data from [18]).

platform [25]. Beams and columns of the steel MRF are represented with an elastic element. The nonlinear response of the same components is simulated with two concentrated plasticity springs at the ends of the elastic elements. These springs follow the hysteretic response of the modified Ibarra–Krawinkler deterioration model including fracture due to low cycle fatigue. Available experimental data [10] for steel beam-to-column subassemblies of the specimen were used to simulate component deterioration and fracture. A comparison between the simulated and experimental hysteretic response of one of those connections is shown in Fig. 7a and b, respectively. As seen from Fig. 7, the component model is able to represent fairly well the hysteretic response of the steel beam-to-column connection of the test specimen till fracture occurs. The implication of fracture in the numerical model is that the bending strength of the steel beam drops to zero in the loading direction that fracture occurs.

The flexibility of the panel zone including panel zone shear distortion is simulated with the Krawinkler model as proposed in [47]. However, based on the shaking table test results, no inelastic behavior was observed in the panel zones. The concrete layers at the top of the steel structure were represented with "rigid" elements in the analytical model of the test frame. The rubber bearings at each concrete layer were modeled with a parallelogram model that deforms in shear. Steel dampers between the concrete layers were modeled with a bilinear model. This model was calibrated with experimental data released from the steel damper manufacturer. Second order effects (P-Delta) were considered in the numerical simulation with OpenSees. Rayleigh damping ratios were assumed to be 2.6% and 4.7% for the first and third mode, respectively. The numerical model of the steel MRF in the longitudinal loading direction was subjected to the same earthquake sequence discussed in Section 3.1. Cumulative damage effects from phase to phase were also considered.

4.1. Results and discussion

This section discusses the main observations obtained from the seismic response of the test specimen during the sequential ground motion shaking. These observations are based on a comparison between numerical simulations versus measured experimental data of the test specimen. The emphasis is on the last phase of the testing sequence (San3) discussed in Section 3.1. During this phase, fractures due to low cycle fatigue occurred at the floor beams of the bottom stories of the steel MRF in the longitudinal direction.

The simulated and measured peak story drift ratio (SDR) profile along the height of the test frame for the ElCentro wave is shown in Fig. 8a. From this figure it is notable that both analytical and measured data are well correlated. During this earthquake record (Level 2 earthquake in Japan) the maximum SDRs did not exceed 1% radians. This indicates that the structure complies with the Japanese seismic code for Level 2 earthquakes. Fig. 8b illustrates the SDR profile along the height of the steel MRF during San3 wave as predicted by analysis with/without fracture. Superimposed is the measured SDR response during the earthquake simulator test

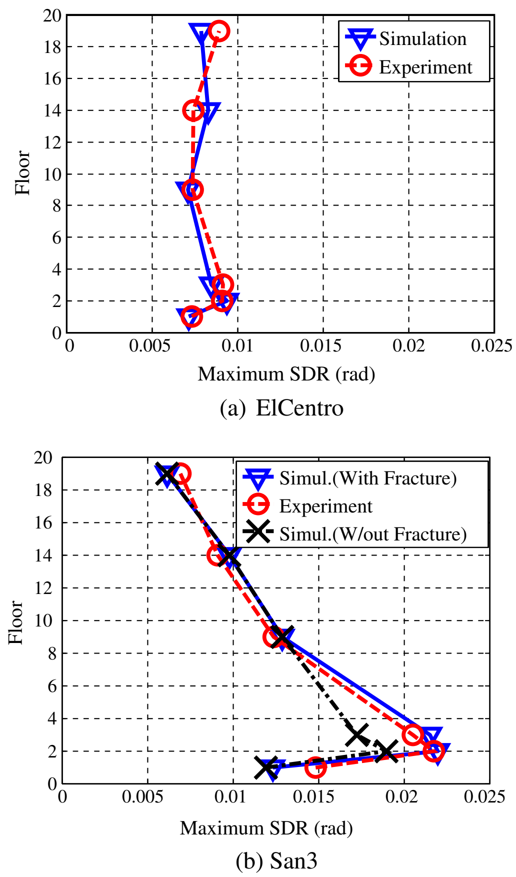

Fig. 8. Maximum story drift ratios along the height of the steel frame in longitudinal direction for ElCentro and San3 seismic waves.

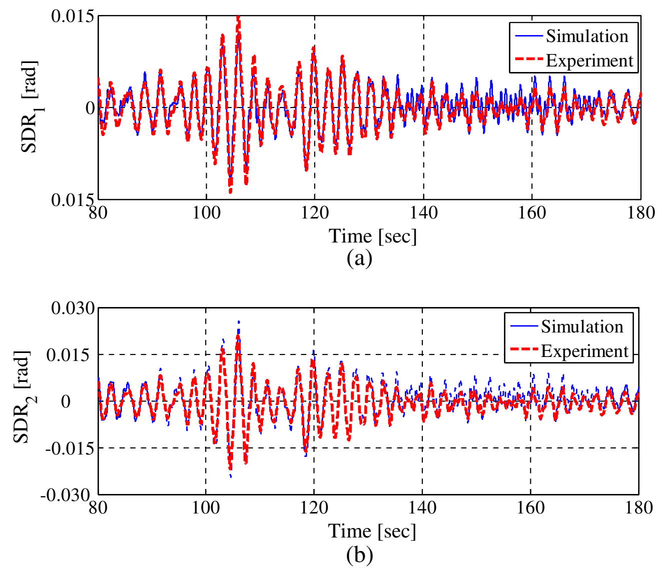

Fig. 9. Comparison of simulated versus experimental response of story drift ratios at first and second story of the test frame during San3 (experimental data from [18]).

in the longitudinal direction. From this figure, the SDR distribution profile of the San3 long period long duration ground motion exceeds 2% radians at the bottom stories and migrates to the top stories. This drift profile along the height of the test frame agrees with an extensive number of analytical studies on high-rise steel MRFS as discussed in [8,47,48]. From the same figure, it is also evident that fracture modeling is critical for accurate representation of dynamic response of the high-rise steel structure at the bottom stories. During the earthquake simulator test, SDRs are amplified due to two beam fractures at the 2nd and 3rd floor beams. The fractures occurred on the right side of both beams. The numerical model seems to underestimate the peak SDRs in the first story of the test frame. However, after looking carefully at a 100 s time window of the overall first story drift history during San3 wave (see Fig. 9a), it is indicated that there is satisfactory correlation between simulated and measured story drift history response. The same observation can be made for the 2nd story drift ratio history, which is shown in Fig. 9b. From the same figure, it is also observed that the overall post-fracture response of the test frame is predicted fairly well with the component model, which proposed in this paper. The difference of the simulated response of the 2-D model compared to the experimental data after fractures occur is attributed to torsional effects that were observed during the shaking table test series after the occurrence of fractures [18]. The torsional effects were not considered in the 2-D modeling of the steel MRF. Another reason for the observed differences is that the numerical model discussed in Section 2.1 is not able to simulate the remaining bending capacity of a steel beam after the occurrence of the first fracture.

4.2. Effect of fracture on the remaining seismic capacity of the high-rise steel building

After completion of the San3 wave two steel beam-to-column connections of the test specimen in the longitudinal direction are fractured. Due to safety reasons the shaking table test series stopped. However, the numerical model discussed in this paper allows for further investigation of the effect of fractured connections on the seismic capacity of the steel MRF, since the experimental results from the earthquake simulator tests were replicated fairly well up to San3 wave. The numerical model of the steel MRF in the longitudinal direction is subjected to a fourth San wave (noted as San4). Cumulative damage effects from the ElCentro, Hog and San1 to San3 waves are simulated. Fig. 10 shows the peak story drift ratios along the height of the high-rise building after zooming at the first 3-stories of interest. For reference, we have superimposed the measured peak SDR profile from San3 wave. From the same figure it can be seen that the peak SDR in the 2nd story of the steel MRF exhibits 3% rad. The amplification of the 2nd story drift ratios during San4 is attributed to sequential fracture of the steel beam connections in the same story due to moment redistribution. In the same figure we have superimposed the peak SDR profile of the same steel MRF when fracture is not simulated in the numerical model. The seismic response of the steel MRF is clearly underestimated by more than 50% in terms of SDRs. This indicates that modeling of fracture due to low cycle fatigue is critical in order to estimate the post-fracture seismic capacity of a high-rise steel building subjected to long period long duration ground motions. P-Delta effects at the bottom stories of the steel MRF are amplified due to large story drift ratios. P-Delta effects dominate the seismic response of a high-rise steel building in the highly inelastic range and typically lead to a collapse mechanism that involves only the bottom stories of a steel building. This has also been pointed out by other analytical studies [21,47,48].

5. Numerical model limitations

This section discusses limitations of the proposed phenomenological model that simulates fracture due to low cycle fatigue. After

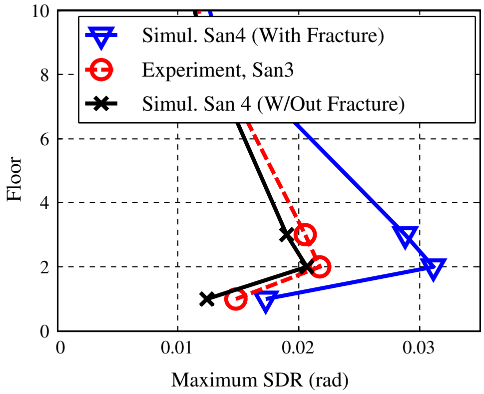

Fig. 10. Maximum story drift ratios along the height of the steel frame during simulated San4 (Level 3) intensity (experimental data from [18]).

beam-to-column connection fractures occur, the bending strength of the steel component that fractures drops to zero based on the numerical model discussed in this paper. However, based on the post-fracture hysteretic response of a steel component there is a remaining bending capacity due to web and flange resistance that has not fractured yet (see Fig. 7b). Because of limited experimental data related to post-fracture performance of WUF connections it is not possible to quantify the remaining bending capacity of a steel beam after the occurrence of the first fracture. Most of the beam-to-columns tests conducted in the past stop due to safety issues after the occurrence of the first fracture during the monotonic or cyclic response. Another limitation of the proposed model is that it is not able to accurately simulate the hysteretic response of bolted steel connections. The primary problem in this case is that the hysteretic response of a bolted connection becomes pinched if a bolt or a number of bolts slip.

6. Conclusions

This paper proposes a numerical model that simulates component deterioration and fracture due to low cycle fatigue of steel beam-to-column connections. Fracture due to low cycle fatigue is expressed with respect to the dissipated energy of a steel component when subjected to cyclic loading. The proposed numerical model has been implemented in a widely used open source numerical simulation platform. This model is particularly useful for quantification of the seismic capacity of high-rise steel buildings subjected to long period long duration ground motions. Component deterioration and fracture in this case is profound due to large number of inelastic deformations. The main findings in this paper are summarized as follows:

1. The number of cycles to fracture for a steel component with respect to its dissipated energy during cyclic loading follows a power law. It was shown that the exponent of this relationship could be kept as a constant. A set of beam-to-column connections that fail in a ductile manner was utilized for this purpose.
2. After validation of the proposed numerical model with landmark experimental data from a recently conducted full scale shaking table test of a high-rise steel building at the world's largest earthquake simulator at E-Defense, it was shown that connection fractures due to cumulative damage amplify maximum story drift ratios at lower stories of high rise buildings. Post-fracture response is significantly underestimated if deterioration and connection fractures are not simulated in the nonlinear dynamic analysis.
3. After connection fractures occur during dynamic loading, story drift ratios at the bottom stories of a high-rise building amplify due to sequential fracture that occurs due to moment redistribution of the steel components.

The main limitation of the proposed numerical model that simulates fracture due to low cycle fatigue is that it is not able to simulate the post-fracture remaining bending capacity of a steel connection after the occurrence of the first fracture.

Acknowledgements

This study was based on work supported by a post-doctoral research fellowship from the Japan Society for the Promotion of Science (award number P09291) awarded to the first author. The financial support is gratefully acknowledged. Any opinions, findings, and conclusions or recommendations expressed in this paper are those of the authors and do not necessarily reflect the views of the sponsors.

References

[1] FEMA-355E. State of the art report on past performance of steel moment – frame buildings in earthquakes. Prepared by the SAC Joint venture for the federal emergency management agency, Washington, DC; 2000.
[2] Nakashima M, Inoue K, Tada M. Classification of damage to steel buildings observed in the 1995 Hyogoken-Nanbu earthquake. J Eng Struct 1998;20(4–6):271–81.
[3] Cornell CA, Luco N. The effects of connection fractures on steel moment resisting frame seismic demands and safety: Report number SAC-BD/99-03, SAC joint venture, Sacramento, California; 1999.
[4] Maison BF, Kasai K. Analysis of Northridge damaged thirteen-story WSMF building. Earthq Spectra 1997;13(3):451–73.
[5] Mahin SA, Morishita K. The effect of strength deterioration on the dynamic response of simple systems subjected to impulsive loading. In: Proceedings of the US–Japan workshop on near-field earthquake damage in urban areas. Earthquake Engineering Research Laboratory. California Institute of Technology, Pasadena, California, 1998.
[6] Lee K, Foutch DA. Seismic performance evaluation of pre-Northridge steel frame buildings with brittle connections. ASCE, J Struct Eng 2002;128(4):546–55.
[7] SAC joint venture. Recommended seismic design criteria for new steel moment frame buildings. Report number FEMA 350, Federal Emergency Management Agency, Washington, DC; 2000.
[8] Nakashima M, Roeder CW, Maruoka Y. Steel moment frames for earthquakes in United Stated and Japan. ASCE, J Struct Eng 2000;126(8):861–8.
[9] Japan Society of Civil Engineering. Architectural Institute of Japan. Report of seismic performance improvement of civil, architectural structures subjected to long-period ground motions generated by subduction zone; 2006 [in Japanese].
[10] Chung Y, Nagae T, Matsumiya T, Nakashima M. Seismic resistance capacity of beam-column connections in high-rise buildings: E-Defense shaking table test. J Earthq Eng Struct Dyn; 2010. doi:10.1002/eqe.1037.
[11] Barsom J, Pellegrino J. Failure analysis of welded steel moment-resisting frame connections. J Mater Civil Eng 2002;14(1):24–34.
[12] Stojadinovic B. Stability and low-cycle fatigue limits of moment connection rotation capacity. J Eng Struct 2004;25:691–700.
[13] Ricles JM, Mao C, Lu LW, Fisher JW. Development and evaluation of improved details for ductile welded unreinforced flange connections. Report number SAC/BD-00/24, SAC Joint Venture, Sacramento, California; 2000.
[14] Plumier A, Agatino MR, Castelllani A, Castiglioni CA, Chesi C. Resistance of steel connections to low-cycle fatigue. In: Proceedings of the 11th European conference on earthquake engineering. Rotterdam: Balkema; 1998.
[15] Machizuki K, Obana L. Seismic activities along the Nankai trough. Bull Earthq Res Inst Univ Tokyo 2003;78:185–95.
[16] Kamae K, Kawabe H, Irikura K. Strong ground motion prediction for huge subduction earthquakes using a characterized source model and several simulation techniques. In: Proceedings of the 13th world conference earthquake engineering, Vancouver, BC, Canada; 2004. p. 655–66.
[17] Boroschek R, Soto P, Leon R, Comte D. Preliminary acceleration information for the Chilean earthquake in February 27th, 2010. Report number 3 (1), University of Chile, Santiago, Chile; 2010.
[18] Chung Y, Nagae T, Hitaka T, Nakashima M. Seismic resistance capacity of high-rise buildings subjected to long-period ground motions: E-Defense shaking table test. ASCE, J Struct Eng 2010;136(6):637–44.
[19] Suita K, Kitamura Y, Goto T, Iwata T, Kamae K. Seismic response of high-rise buildings constructed in 1970s subjected to long-period ground motions. J Struct Constr Eng, Archit Inst Jpn 2007;611:055–61.

[20] Nakashima M, Minami T, Mitani I. Moment redistribution caused by beam fracture in steel moment frames. ASCE, J Struct Eng 2000;126(1):137–44.
[21] Luco N, Cornell A. Effects of connection fractures on SMRF seismic drift demands. ASCE, J Struct Eng 2000;126(1):127–36.
[22] Rodgers J, Mahin S. Effects of connection fractures on global behavior of steel moment frames subjected to earthquakes. ASCE, J Struct Eng 2006;132(1):78–88.
[23] Nakashima M, Matsumiya T, Suita K, Zhou F. Full-scale test of composite frame under large cyclic loading. ASCE, J Struct Eng 2007;133(2):297–304.
[24] Nagae T, Kajiwara K, Inoue T, Nakashima M. Large scale shaking table tests for high-rise buildings: new projects of E-Defense Chapter 43: Advances in performance-based earthquake engineering. In: Fardis MN, editor. Geotechnical, geological, and earthquake engineering, vol. 13. Springer; 2010.
[25] McKenna F. Object oriented finite element programming frameworks for analysis, algorithms and parallel computing. PhD thesis, University of California, Berkeley, California; 1997.
[26] Bertero V, Popov E. Effects of large alternating strains of steel beams. ASCE, J Struct Div 1965;91:ST1.
[27] Park Y, Ang A, Wen Y. Stochastic model for seismic damage assessment. In: ASCE proceedings of the 5th engineering mechanics division specialty conference; 1984. p. 1168–71.
[28] Krawinkler H, Zohrei M, Irvani BL, Cofie N, Tamjed HH. Recommendations for experimental studies on the seismic behavior of steel components and materials. Report number 61, the John. A. Blume Earthquake Engineering Research Center, Department of Civil Engineering, Stanford University; 1983.
[29] Manson SS. Fatigue, a complex subject: some simple approximations. J Exp Mech 1965;5:193–226.
[30] Uriz P, Fillipou FC, Mahin SA. Model for cyclic inelastic buckling of steel braces. ASCE, J Struct Eng 2008;134(4):619–28.
[31] Krishnan S. Modified Elastofiber element for steel slender column and brace modeling. ASCE, J Struct Eng 2010;136(11):1350–66.
[32] Kanvinde AM, Deierlein GG. Void growth model and stress modified critical strain model to predict ductile fracture in structural steels. ASCE, J Struct Eng 2006;132(2):1907–18.
[33] Kanvinde AM, Deierlein GG. Validation of cyclic void growth model for fracture initiation in blunt notch and dogbone steel specimens. ASCE, J Struct Eng 2008;134(9):1528–37.
[34] Kanvinde AM, Deierlein GG, Myers AT. Experimental investigation of inelastic cyclic buckling and fracture of steel braces. ASCE, J Struct Eng 2009;135(9):19–32.
[35] Lin X, Okazaki T, Chung Y, Nagae T, Matsumiya T, Nakashima M. Retrofit evaluation on local fracture failure of welded moment-resisting connection. In: Proceedings of the Architectural Institute of Japan, Tsukuba, Japan; 2010.
[36] Lee K, Stojadinovic B. Low-cycle fatigue limit on seismic rotation capacity for US Steel moment connections. In: Proceedings of the 13th world conference on earthquake engineering, Vancouver, Canada; 2004.
[37] Campbell SD, Richard RM, Partridge JE. Steel moment frame damage predictions using low-cycle fatigue. In: Proceedings of the 14th world conference on earthquake engineering, Beijing, China; 2008.
[38] Ibarra LF, Medina RA, Krawinkler H. Hysteretic models that incorporate strength and stiffness deterioration. J Earthq Eng Struct Dyn 2005;34(12):1489–511.
[39] Lignos DG, Krawinkler H. Sidesway collapse of deteriorating structural systems under seismic excitations. Report number 172, the John A. Blume Earthquake Engineering Research Center, Department of Civil Engineering, Stanford University; 2009.
[40] Rahnama M, Krawinkler H. Effect of soft soils and hysteresis models on seismic design spectra. Report number 108, the John A. Blume Earthquake Engineering Research Center, Department of Civil Engineering, Stanford University; 1993.
[41] Lignos DG, Krawinkler H. A database in support of modeling of component deterioration for collapse prediction of steel frame structures. ASCE, Proceedings of the structures congress, Long Beach CA: SEI institute; 2007.
[42] American Institute of Steel Construction, Inc. Seismic provisions for structural steel buildings; March 2005.
[43] Lignos DG, Billington SL. Hybrid testing of a retrofitted steel moment resisting frame with infill panels. In: Proceedings of the 9th US national and 10th Canadian conference on earthquake engineering, Toronto, Canada; 2010.
[44] Dennis JE Jr. Nonlinear least-squares, state of the art in numerical analysis. In: Jacobs D. editor. Academic Press; 1977. p. 269–312.
[45] Moré JJ. The Levenberg–Marquardt algorithm: implementation and theory, numerical analysis. In: Watson GA, editor. Lecture notes in mathematics, vol. 630. Springer; 1977. p. 105–16.
[46] Kuwamura H, Takagi N. Similitude law of prefracture hysteresis of steel members. ASCE, J Struct Eng 2004;130(5):752–61.
[47] Gupta A, Krawinkler H. Prediction of seismic demands for SMRFs with ductile connections and elements. Report No. SAC/BD-99/06, SAC Background Document; 1999.
[48] ATC-76-1. Quantification of building system performance and response parameters. FEMA Report 90% draft, Applied Technology Council; 2010.